

1  
2  
3  
4  
5  
6  
7 In this study, we identified anti-PDI-antibody immunopositive NCIs in the  
8  
9  
10 spinal cord of patients with ALS. Furthermore, we found PDI-immunopositive swollen  
11  
12 neurites in the spinal cord of patients with ALS. In addition, TDP-43 and SOD1 were  
13  
14 co-localized with PDI in NCIs of patients with ALS. The accumulation of misfolded  
15  
16 proteins such as SOD1 and TDP-43 is toxic for motor neurons and PDI may be involved  
17  
18  
19  
20  
21  
22 in NCIs.  
23  
24  
25  
26  
27  
28  
29

## 30 31 **Material and Methods**

### 32 33 34 *Tissue preparation*

35  
36  
37 Postmortem spinal cord specimens from five patients with SALS and one with FALS  
38  
39 (I113T), and five normal control were utilized in this study. All patients gave informed  
40  
41 consent and this study was approved by the local ethics committee. The diagnosis of the  
42  
43 patients was defined by pathological study. Specimens from the spinal cord and  
44  
45 brainstem were obtained from the autopsied spinal cord of the normal control and ALS  
46  
47 patients. All samples were fixed in 10% neutral formalin at room temperature. Several  
48  
49 paraffin-embedded tissue blocks were prepared and cut into 7  $\mu$ m-thick sections on a  
50  
51 microtome. The paraffin-embedded sections were deparaffinized in xylene, followed by  
52  
53  
54  
55  
56  
57  
58  
59  
60

1  
2  
3  
4  
5  
6  
7 rehydration in ethanol solutions of decreasing concentration as previously described  
8  
9  
10 (9,10).

### 16 *Immunohistochemistry*

17  
18 Immunohistochemical staining was performed as previously described (9,10).

19  
20  
21  
22 Immunohistochemical staining for PDI was performed using polyclonal rabbit anti-PDI  
23  
24  
25 antibody that has been described before (11-13). Monoclonal mouse anti-TDP-43  
26  
27  
28 antibody was purchased from Abnova (Taipei, Taiwan) and mouse anti-human SOD1  
29  
30  
31 antibody was purchased from R&D systems, Inc. (Minneapolis, MN, USA). The  
32  
33  
34 sections were incubated in a microwave oven for a few minutes after which the sections  
35  
36  
37 were incubated in 0.3% hydrogen peroxide in 0.1 M PBS at room temperature for 30  
38  
39  
40 min to block the endogenous peroxidase activity. After washing with PBS containing  
41  
42  
43 0.3% Triton X100 (PBST) the sections were incubated overnight with the primary  
44  
45  
46 antibody diluted in PBST at room temperature. A dilution of 1:100 was used for the  
47  
48  
49 primary PDI antibody. After incubation with the primary antibody and washing, the  
50  
51  
52 sections were incubated with the secondary antibody (diluted 1:100). The sections were  
53  
54  
55 incubated with an avidin biotin complex, and were allowed to react with a solution  
56  
57  
58 containing 0.02% 3,3'-diaminobenzidine tetrahydrochloride (DAB), 0.005% hydrogen  
59  
60

1  
2  
3  
4  
5  
6  
7 peroxide, and 0.6% nickel acetate in 0.05 M Tris/HCl buffer.  
8  
9

10  
11  
12  
13 *Double staining of PDI and human TDP-43 in tissue sections from SALS samples*  
14

15  
16 To confirm the anatomical relationship between PDI and human TDP-43, we performed  
17  
18 a double-staining study using mouse anti-TDP-43 antibody and rabbit anti-PDI antibody  
19  
20 as described in (9). Briefly, sections of the spinal cords were incubated in medium  
21  
22 containing anti-TDP-43 and anti-PDI antibodies (each diluted 1:100) in PBST overnight  
23  
24  
25 containing anti-TDP-43 and anti-PDI antibodies (each diluted 1:100) in PBST overnight  
26  
27  
28 at room temperature. After washing, the sections were reacted with the secondary  
29  
30  
31 antibodies consisting of polyclonal goat anti-rabbit immunoglobulins/FITC (The  
32  
33 Jackson Laboratory, Bar Harbor, ME, USA) and polyclonal swine anti-mouse  
34  
35 immunoglobulins/TRITC (Cosmo Bio Science, San Diego, CA, USA) for 1 h at room  
36  
37  
38 temperature. After rinsing, the slides were mounted Vectashield (Vector Laboratories,  
39  
40  
41 Burlingame, CA, USA) and photographed using an Olympus Fr1000D: FV/IX81  
42  
43  
44 (Olympus corporation, Tokyo, Japan) confocal laser scanning microscope. We selected  
45  
46  
47 15 TDP-43-immunopositive NCIs in the immunostained sections of the spinal cord  
48  
49  
50 from each of three patients with SALS. We then counted the number of  
51  
52  
53 PDI-immunopositive NCIs in the selected TDP-43-immunopositive NCIs from each  
54  
55  
56  
57  
58  
59 patient.  
60

1  
2  
3  
4  
5  
6  
7  
8  
9  
10 *Double staining of PDI and SOD1 in FALS samples*

11  
12 Double staining using anti-PDI antibody and anti-SOD1 antibody was performed as  
13  
14 described above. We selected 15 SOD1-immunopositive NCIs in the immunostained  
15  
16 sections of the spinal cord from the patient with FALS. We then counted the number of  
17  
18 PDI-immunopositive NCIs in the selected SOD1-immunopositive NCIs from the  
19  
20 patient.  
21  
22  
23  
24  
25  
26  
27  
28  
29

30  
31 **Results**

32  
33 *PDI-immunopositive neuronal cells*

34  
35 In the control specimens, many neurons were immunopositive for the anti-PDI antibody.  
36  
37  
38 PDI immunoreactivity was typically observed in the neuronal bodies and dendrites, but  
39  
40 nuclei were not stained (Figure 1, panels A,B). In addition, some of the  
41  
42 oligodendrocytes were also immunopositive using anti-PDI antibody (Figure 1, panel B).  
43  
44  
45 Some of astrocytes were PDI-immunopositive, but they were stained weakly. In the  
46  
47 tissue sections from patients with SALS and FALS, we detected numerous  
48  
49 PDI-immunopositive NCIs (Figure 2, panels A,B). These PDI-immunopositive NCIs  
50  
51  
52 were observed in all patients with SALS and FALS. Furthermore, we found  
53  
54  
55  
56  
57  
58  
59  
60

1  
2  
3  
4  
5  
6  
7 anti-PDI-antibody-immunopositive swollen neurites in SALS and FALS samples  
8  
9  
10 (Figure 3, panels A,B). Other immunoreactivity of anti-PDI antibody was not markedly  
11  
12  
13 different between the normal and ALS patients.  
14  
15  
16  
17

#### 18 *Double staining of PDI and TDP-43 in SALS samples*

19  
20  
21  
22 Immunohistochemical double staining for PDI and TDP-43 showed that PDI and  
23  
24  
25 TDP-43 were co-localized in the NCIs of SALS samples (Figure 4). The number of  
26  
27  
28 NCIs labeled by antibodies to PDI was smaller than the number of  
29  
30  
31 TDP-43-immunopositive NCIs (Figure 4). A quantitative examination revealed that  
32  
33  
34 approximately 93% of the TDP-43-immunopositive NCIs were also  
35  
36  
37 PDI-immunoreactive. The proportion of PDI-immunopositive NCIs compared with  
38  
39  
40 TDP-43-immunopositive NCIs was not remarkably different among patients.  
41  
42  
43  
44  
45  
46

#### 47 *Double staining of PDI and SOD1 in FALS samples*

48  
49  
50 Immunohistochemical double staining for PDI and SOD1 showed that PDI and SOD1  
51  
52  
53 were co-localized in the NCIs of FALS samples (Figure 5). The number of NCIs labeled  
54  
55  
56 by antibodies to PDI was less than the number of SOD1-immunopositive NCIs. A  
57  
58  
59 quantitative examination revealed that approximately 73% of the  
60

1  
2  
3  
4  
5  
6  
7 SOD1-immunopositive NCIs were also PDI-immunoreactive.  
8  
9

## 10 11 12 **Discussion**

13  
14  
15  
16 The accumulation of misfolded, aggregated proteins and  $\text{Ca}^{2+}$  influx can cause  
17  
18 ER stress in neurons (5). ER stress signaling, otherwise known as the unfolded protein  
19  
20 response (UPR), is triggered by an increased load of misfolded proteins in the organelle.  
21  
22 In SOD1 (L84V) transgenic mice, the aggregation of ER and numerous free ribosomes  
23  
24 was observed associated with abnormal inclusion-like structures in spinal cord neurons  
25  
26 at the presymptomatic stage (14). Furthermore, the induction of LBHIs *in vitro* by ER  
27  
28 stress in neuroblastoma cells was revealed and the inclusions were closely similar to  
29  
30 LBHIs in patients with SOD1-linked FALS (14). The accumulation of SOD1 can cause  
31  
32 ER stress and that may cause apoptosis of neuronal cells in FALS.  
33  
34  
35  
36  
37  
38  
39  
40  
41  
42

43  
44 Mutant SOD1 specifically interacted with Derlin-1, a component of  
45  
46 ER-associated degradation (ERAD) machinery and triggered ER stress through  
47  
48 dysfunction of ERAD (15). Mutant SOD1-induced ER stress activated apoptosis.  
49  
50 Perturbation of binding between mutant SOD1 and Derlin-1 by Derlin-1-derived  
51  
52 oligopeptide suppressed mutant SOD1-induced ER stress and motor neuron death (15).  
53  
54  
55  
56  
57  
58 In addition, Derlin-1 overexpression reduced mutant SOD1-induced cell toxicity and  
59  
60

1  
2  
3  
4  
5  
6  
7 increased cell viability by suppressing the activation of the ER stress pathway factors  
8  
9  
10 (16). Interestingly, exogenous Derlin-1 resulted in a decrease in the amount of mutant  
11  
12 SOD1, and a lesser decrease in that of wild-type SOD1 in transfected cells. In addition,  
13  
14 reduced SOD1 protein expression was observed in the microsomal fraction of wild-type  
15  
16 and mutant SOD1 cells (16). Furthermore, Chromogranins, components of  
17  
18 neurosecretory vesicles, interact with mutant forms of SOD1 that are linked to ALS, but  
19  
20 not with wild-type SOD1 (17). These results suggest that Derlin-1 and Chromogranins  
21  
22 may act as chaperone-like proteins to promote the secretion of SOD1 mutants. In ALS,  
23  
24 the mutant SOD1-binding protein could play an important role through the ER stress  
25  
26 pathway. There are a lot of ER-related chaperone proteins in neurons. In these proteins,  
27  
28 Derlin-1 and Chromogranin bind to mutant SOD1. These two proteins may be the link  
29  
30 to co-localization of mutant SOD1 and PDI.  
31  
32  
33  
34  
35  
36  
37  
38  
39  
40  
41  
42

43 PDI is an ER-specific chaperone and is linked to the accumulation of misfolded  
44  
45 proteins in many neurodegenerative diseases (5). In this study, we have shown the  
46  
47 localization of PDI in neuronal cells. PDI prevents the neurotoxicity associated with ER  
48  
49 stress and protein misfolding, but NO blocks the enzyme's protective effect through the  
50  
51 S-nitrosylation of PDI. This inhibition of PDI leads to ER stress, which can induce  
52  
53 apoptosis (5). Recently, S-nitrosylation of PDI in patients with ALS was reported (8).  
54  
55  
56  
57  
58  
59  
60

1  
2  
3  
4  
5  
6  
7 The levels of S-nitrosylated PDI were increased in transgenic mutant SOD1 mouse and  
8  
9  
10 human SALS spinal cord tissues. Hence, despite upregulation, PDI is also functionally  
11  
12  
13 inactivated in ALS (8). NO-induced S-nitrosylation of PDI inhibits its enzymatic  
14  
15  
16 activity, leading to the accumulation of polyubiquitinated proteins in ALS model mice  
17  
18  
19 (8). Furthermore, overexpression of PDI decreased mutant SOD1 aggregation, inclusion  
20  
21  
22 formation, ER stress induction, and toxicity, whereas small interfering RNA targeting  
23  
24  
25 PDI increased mutant SOD1 inclusion formation, indicating a protective role for PDI  
26  
27  
28 against SOD1 misfolding (8). Thus, PDI prevents the neurotoxicity associated with ER  
29  
30  
31 stress and misfolding in ALS. In addition, PDI was present in cerebrospinal fluid and  
32  
33  
34 was aggregated and widely distributed throughout the motor neurons of patients with  
35  
36  
37 SALS (18).

38  
39  
40  
41 The accumulation of SOD1 is a link to the pathogenesis of FALS (3).

42  
43  
44 Nevertheless, the accumulation of SOD1 is not observed in SALS. The mechanism of  
45  
46  
47 SALS may be different from FALS. TDP-43 is the major component of LBHIs and  
48  
49  
50 TDP-43 is seen in patients with SALS, but TDP-43 is not the only protein to contribute  
51  
52  
53 to the pathology of SALS. Further study is needed to elucidate the mechanism of  
54  
55  
56  
57 progressive accumulation of TDP-43 in neurons.  
58  
59  
60



1  
2  
3  
4  
5  
6  
7 Another pathological hallmark of ALS is swollen neurites. Axonal transport has  
8  
9  
10 two components: transport of vesicles and mitochondria by kinesin and related  
11  
12 proteins (fast transport) and movement of the major structural components of the  
13  
14 neuron, many enzymes, and other cytoplasmic proteins (slow transport). Slow  
15  
16 transport can be divided into two components based on the rate of movement and  
17  
18 containing the neurofilament proteins tubulin and actin, and containing tubulin, actin,  
19  
20 and other cytoplasmic proteins (19). Retardation of slow axonal transport is a very  
21  
22 early event in mice expressing the FALS-linked SOD1 (G37R) and SOD1 (G85R)  
23  
24 mutations (19). In SOD1 (G85R) mutant mice, this is the earliest known abnormality,  
25  
26 arising months before any pathological changes can be detected. Tubulin transport  
27  
28 slows more dramatically at earlier stages, whereas the transport of neurofilaments and  
29  
30 other cargo yet to be identified is affected at later time points, indicating a worsening  
31  
32 of the defect, and presumably the underlying neuronal health and function, with time.  
33  
34 This is consistent with the slow accumulation of damage over a long period, ultimately  
35  
36 culminating in late onset of disease in both mice and humans. Further support for a  
37  
38 disruption in slow axonal transport early in disease comes from the obvious proximal  
39  
40 axon swellings in both SOD1 (G37R) and SOD1 (G85R) mice (19). The known  
41  
42 neurofilament dependent slowing of axonal transport, combined with the accumulation  
43  
44  
45  
46  
47  
48  
49  
50  
51  
52  
53  
54  
55  
56  
57  
58  
59  
60

1  
2  
3  
4  
5  
6  
7 of neurofilaments in ALS, suggests that an important aspect of toxicity may arise from  
8  
9  
10 damage to transport (19).

11  
12  
13  
14 In this study, we have revealed anti-PDI-antibody-immunopositive NCIs in the  
15  
16 patients with SALS and FALS. Furthermore, PDI was co-localized with TDP-43 and  
17  
18 SOD1 in NCIs. We assume that NO inhibited PDI and led to the accumulation of  
19  
20 unfolded proteins in ALS. Abnormal TDP-43 and SOD1 or other proteins may be  
21  
22 accumulated in NCIs and cause ER stress in ALS. In degenerated motor neurons, ER  
23  
24 and other organelles are probably destroyed and injured. As PDI is working in neurons  
25  
26 as a chaperone it may bind to TDP-43 or SOD1, and become included in NCIs. But the  
27  
28 PDI in the NCIs may be a non-functional protein. We propose the mechanism of action  
29  
30 of PDI recruitment to NCIs to be as follows. First, many unfolded proteins can  
31  
32 accumulate in both cytosol and ER lumen of the motor neurons of patients with ALS,  
33  
34 and these unfolded proteins can accumulate and make a mass of accumulated unfolded  
35  
36 proteins. Second, this mass disrupts the organelle compartment, and as a result, many  
37  
38 chaperone proteins including the ER-resident protein PDI, are involved in this mass.  
39  
40 Since these accumulated proteins expose the hydrophobic surface, it is easy for PDI to  
41  
42 interact with these unfolded proteins by hydrophobic interaction. The co-localization of  
43  
44 PDI and TDP-43 or SOD1 in NCIs could be linked to the formation of these inclusions.  
45  
46  
47  
48  
49  
50  
51  
52  
53  
54  
55  
56  
57  
58  
59  
60

1  
2  
3  
4  
5  
6  
7           One of the great puzzles in the study of ALS is why the motor system, and  
8  
9  
10 particular subsets of motor neurons, is selectively targeted for toxicity. Because of the  
11  
12 accumulation of misfolding proteins, axon transport may be disturbed and make  
13  
14 swollen neurites. As the motor neuron is the longest cell in the human nervous system,  
15  
16  
17 the motor system may be selectively disordered by the accumulation of misfolding  
18  
19 proteins. We observed PDI-immunopositive swollen neurites in the patients with ALS.  
20  
21  
22 PDI may leave the injured ER and become to be aggregated in swollen axons due to  
23  
24  
25 disturbance of axon transport. In the ALS model mouse, axonal swelling is one of the  
26  
27  
28 early events and PDI is accumulated in the swollen axons in human ALS samples.  
29  
30  
31  
32 However, further study is needed to find out weather it is a primary event or a late  
33  
34  
35  
36  
37  
38  
39  
40  
41  
42  
43  
44  
45  
46  
47  
48  
49  
50  
51  
52  
53  
54  
55  
56  
57  
58  
59  
60

1  
2  
3  
4  
5  
6  
7           In summary, we found co-localized inclusions of PDI with mutant SOD1 and  
8  
9  
10 TDP-43 in patients with ALS. The ER-specific chaperone protein PDI may leave the  
11  
12 ER and then accumulate with SOD1 or TDP-43 in the cytosol. Furthermore, we found  
13  
14  
15 PDI-immunopositive swollen neurites in patients with SALS and FALS. As neurites  
16  
17  
18 are parts of the motor neuron, they are also degenerated. PDI may also accumulate in  
19  
20  
21  
22 the swollen neurites due to the disturbance of axon transport. But the function of PDI

1  
2  
3  
4  
5  
6  
7 may be lost. These results suggest that the increase in the PDI activity may be a  
8  
9  
10 promising therapeutic strategy in ALS.  
11

## 12 13 **Acknowledgments**

14  
15  
16 We thank Kumi Kodama and Nana Kawaguchi (Department of Pharmacoepidemiology,  
17  
18  
19  
20  
21  
22  
23  
24  
25  
26  
27  
28  
29  
30  
31  
32  
33  
34  
35  
36  
37  
38  
39  
40  
41  
42  
43  
44  
45  
46  
47  
48  
49  
50  
51  
52  
53  
54  
55  
56  
57  
58  
59  
60  
Kyoto University) for excellent technical assistance. This work was supported in part  
by a research grant from Eijinkai medical group in Japan.

*Declaration of interest:* The authors report no conflicts of interest. The authors  
alone are responsible for the content and writing of the paper.

## References

- (1) Wijesekera LC, Leigh PN. Amyotrophic lateral sclerosis. *Orphanet J Rare Dis.* 2009; 4: 3.
- (2) Reaume AG, Elliott JL, Hoffman EK, Kowall NW, Ferrante RJ, Siwek DF, et al. Motor neurons in Cu/Zn superoxide dismutase-deficient mice develop normally but exhibit enhanced cell death after axonal injury. *Nat Genet.* 1996; 13: 43-7.
- (3) Tu PH, Raju P, Robinson KA, Gurney ME, Trojanowski JQ, Lee VM. Transgenic mice carrying a human mutant superoxide dismutase transgene develop neuronal cytoskeletal pathology resembling human amyotrophic lateral sclerosis lesions. *Proc Natl Acad Sci U S A.* 1996; 93: 3155-60.
- (4) Wegorzewska I, Bell S, Cairns NJ, Miller TM, Baloh RH. TDP-43 mutant transgenic mice develop features of ALS and frontotemporal lobar degeneration. *Proc Natl Acad Sci U S A.* 2009; 106: 18809-14.
- (5) Nakamura T, Lipton SA. Cell death: protein misfolding and neurodegenerative diseases. *Apoptosis.* 2009; 14: 455-68.
- (6) Noiva R, Lennarz WJ. Protein disulfide isomerase. A multifunctional protein resident in the lumen of the endoplasmic reticulum. *J Biol Chem.* 1992; 267: 3553-6.
- (7) Tsai B, Rodighiero C, Lencer WI, Rapoport TA. Protein disulfide isomerase acts as a redox-dependent chaperone to unfold cholera toxin. *Cell.* 2001; 104: 937-48.
- (8) Walker AK, Farg MA, Bye CR, McLean CA, Horne MK, Atkin JD. Protein disulphide isomerase protects against protein aggregation and is S-nitrosylated in amyotrophic lateral sclerosis. *Brain.* 2010; 133: 105-16.
- (9) Honjo Y, Ito H, Horibe T, Takahashi R, Kawakami K. Protein disulfide isomerase-immunopositive inclusions in patients with Alzheimer disease. *Brain Res.* 2010; 1349: 90-6.
- (10) Kawamoto Y, Akiguchi I, Shirakashi Y, Honjo Y, Tomimoto H, Takahashi R, et al. Accumulation of Hsc70 and Hsp70 in glial cytoplasmic inclusions in patients with multiple system atrophy. *Brain Res.* 2007; 1136: 219-27.
- (11) Kimura T, Hosoda Y, Kitamura Y, Nakamura H, Horibe T, Kikuchi M. Functional differences between human and yeast protein disulfide isomerase family proteins. *Biochem Biophys Res Commun.* 2004; 320: 359-65.
- (12) Kimura T, Horibe T, Sakamoto C, Shitara Y, Fujiwara F, Komiya T, et al. Evidence for mitochondrial localization of P5, a member of the protein disulphide isomerase family. *J Biochem.* 2008; 144: 187-96.
- (13) Kimura T, Nishida A, Ohara N, Yamagishi D, Horibe T, Kikuchi M. Functional

1  
2  
3  
4  
5  
6 analysis of the CXXC motif using phage antibodies that cross-react with protein  
7 disulphide-isomerase family proteins. *Biochem J.* 2004; 382:169-76.

8  
9 (14) Yamagishi S, Koyama Y, Katayama T, Taniguchi M, Hitomi J, Kato M, et al. An in  
10 vitro model for Lewy body-like hyaline inclusion/astrocytic hyaline inclusion: induction  
11 by ER stress with an ALS-linked SOD1 mutation. *PLoS One.* 2007; 2: e1030.

12  
13 (15) Nishitoh H, Kadowaki H, Nagai A, Maruyama T, Yokota T, Fukutomi H, et al.  
14 ALS-linked mutant SOD1 induces ER stress- and ASK1-dependent motor neuron death  
15 by targeting Derlin-1. *Genes Dev.* 2008; 22:1451-64.

16  
17 (16) Mori A, Yamashita S, Uchino K, Suga T, Ikeda T, Takamatsu K, et al. Derlin-1  
18 overexpression ameliorates mutant SOD1-induced endoplasmic reticulum stress by  
19 reducing mutant SOD1 accumulation. *Neurochem Int.* 2011; 58:344-53.

20  
21 (17) Urushitani M, Sik A, Sakurai T, Nukina N, Takahashi R, Julien JP.  
22 Chromogranin-mediated secretion of mutant superoxide dismutase proteins linked to  
23 amyotrophic lateral sclerosis. *Nat Neurosci.* 2006; 9:108-18.

24  
25 (18) Atkin JD, Farg MA, Walker AK, McLean C, Tomas D, Horne MK. Endoplasmic  
26 reticulum stress and induction of the unfolded protein response in human sporadic  
27 amyotrophic lateral sclerosis. *Neurobiol Dis.* 2008; 30: 400-7.

28  
29 (19) Williamson TL, Cleveland DW. Slowing of axonal transport is a very early event in  
30 the toxicity of ALS-linked SOD1 mutants to motor neurons. *Nat Neurosci.* 1999; 2:  
31 50-6.

## Figure Legends

### Fig. 1

(A) Neurons (arrows) in normal cervical spinal cord were immunopositive for PDI. (B) Oligodendrocytes (arrowhead) and neurites (arrows) in normal cervical spinal cord were also immunostained by the anti-PDI antibody. Scale bars: 20  $\mu\text{m}$ .

### Fig. 2

Anti-PDI-antibody-immunopositive NCI (arrow) from a patient with (A) SALS (cervical spinal cord) and (B) FALS (cervical spinal cord). Scale bars: 10  $\mu\text{m}$ .

### Fig. 3

(A) Anti-PDI-antibody-immunopositive swollen neurites (arrows) and degenerated neurons (arrowheads) from a patient with FALS (cervical spinal cord). (B) Anti-PDI-antibody-immunoreactive swollen neurites (arrow) from a patient with SALS (cervical spinal cord). Scale bars: 20  $\mu\text{m}$ .

### Fig. 4

Double immunostaining of NCIs from a patient with SALS (cervical spinal cord). TDP-43 and PDI are co-localized in NCIs (arrow). Green: anti-PDI antibody immunostaining (A). Red: anti-TDP-43 antibody immunostaining (B). Yellow: merged

1  
2  
3  
4  
5  
6  
7 immunostaining (C). *Differential interference contrast* (DIC): (D). Scale bar: 20  $\mu\text{m}$ .

8  
9  
10 **Fig. 5**

11  
12 Double immunostaining of NCI from a patient with FALS (cervical spinal cord). SOD1

13  
14 and PDI are co-localized in NCI (arrow). Green: anti-PDI antibody immunostaining (A).

15  
16 Red: anti-SOD1 antibody immunostaining (B). Yellow: merged immunostaining (C).

17  
18  
19  
20  
21  
22 *Differential interference contrast* (DIC): (D). Scale bar: 20  $\mu\text{m}$ .



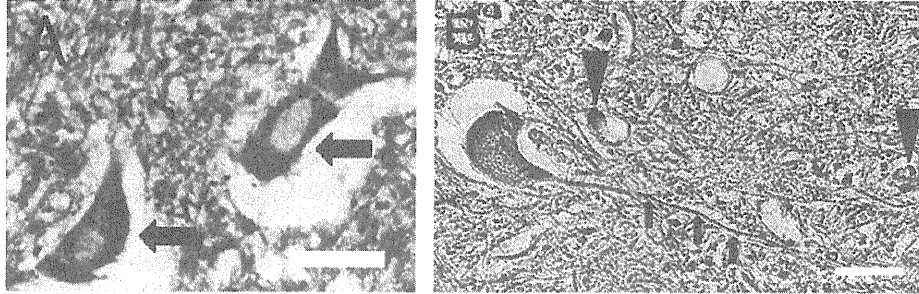


Figure 1

(A) Neurons (arrows) in normal cervical spinal cord were immunopositive for PDI. (B) Oligodendrocytes (arrowhead) and neurite (arrows) in normal cervical spinal cord were also immunostained by the anti-PDI antibody. Scale bars: 20  $\mu$ m.

34x10mm (600 x 600 DPI)

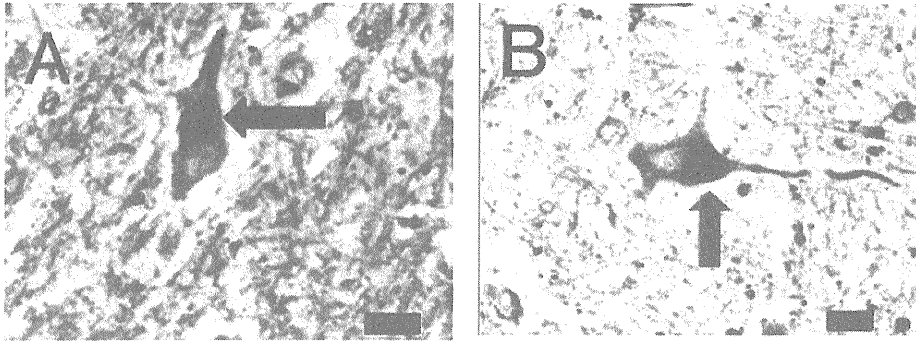


Figure2

Anti-PDI-antibody-immunopositive NCI (arrow) from a patient with (A) SALS (cervical spinal cord) and (B) Anti-PDI-antibody-immunoreactive NCI (arrow) from a patient with FALS (cervical spinal cord). Scale bars: 10  $\mu$ m. 34x12mm (600 x 600 DPI)

1  
2  
3  
4  
5  
6  
7  
8  
9  
10  
11  
12  
13  
14  
15  
16  
17  
18  
19  
20  
21  
22  
23  
24  
25  
26  
27  
28  
29  
30  
31  
32  
33  
34  
35  
36  
37  
38  
39  
40  
41  
42  
43  
44  
45  
46  
47  
48  
49  
50  
51  
52  
53  
54  
55  
56  
57  
58  
59  
60

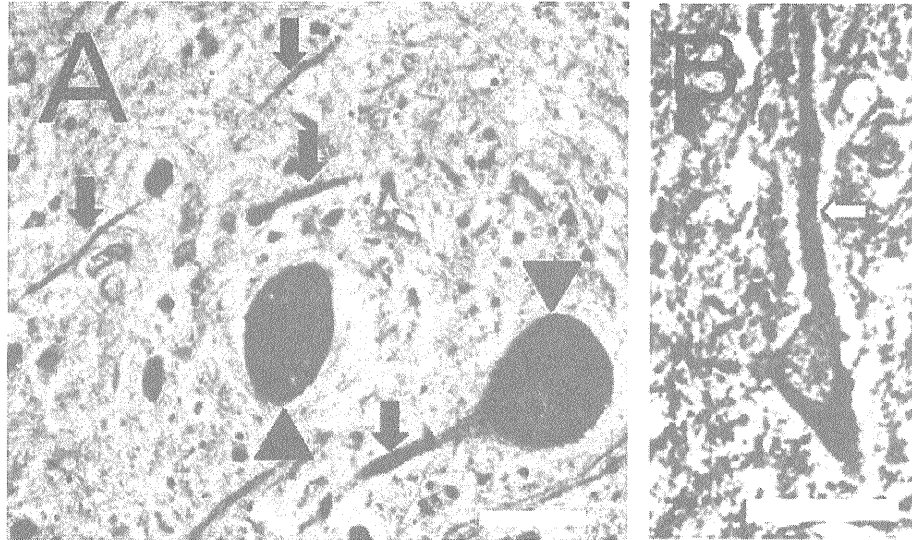


Figure 3  
(A) Anti-PDI-antibody-immunopositive swollen neurites (arrows) and degenerated neurons (arrow heads) from a patient with FALS (cervical spinal cord). (B) Anti-PDI-antibody-immunoreactive swollen neurite (arrow) from a patient with SALS (cervical spinal cord). Scale bars: (A, B) 20  $\mu$ m.

22x13mm (600 x 600 DPI)

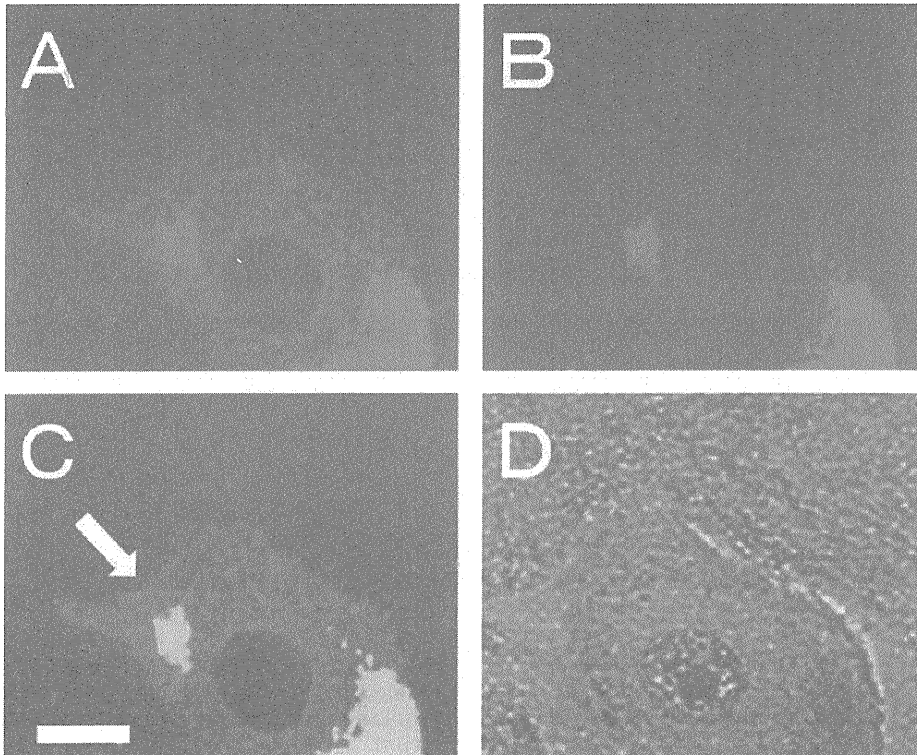


Figure 4

Double immunostaining of NCIs from a patient with SALS (cervical spinal cord). TDP-43 and PDI are co-localized in NCIs (arrow). Green: anti-PDI antibody immunostaining (A). Red: anti-TDP-43 antibody immunostaining (B). Yellow: merged immunostaining (C). Differential interference contrast (DIC): (D). Scale bar: 20  $\mu\text{m}$ .  
54x44mm (600 x 600 DPI)